Pergamon

0301-9322(95)00077-1

Int. J. Multiphase Flow Vol. 22, No. 3, pp. 563–574, 1996

0301-9322/96 $15.00 + 0.00

CLASSIFICATION OF CONCENTRATED SUSPENSIONS USING INCLINED SETTLERS

R. H. DAVIS and H. GECOL

Department of Chemical Engineering, University of Colorado, Boulder, CO 80309-0424, U.S.A.

(Received 11 September 1995; in revised form 15 November 1995)

Abstract—Sedimentation vessels with parallel inclined walls are able to clarify or classify particle suspensions more rapidly than conventional settlers due to their increased surface area and decreased settling distances. The use of continuous inclined settlers to classify or separate particles by size and/or density from concentrated suspensions is considered. Mass balances are applied to each particle species in order to predict its concentration in the settler overflow (fine fraction) and settler underflow (coarse fraction), given the settler geometry, operating conditions, fluid and particle properties, and the particle concentration and size distribution in the feed. A hindered settling function with no adjustable parameters is employed for bidisperse and polydisperse suspensions. Unlike many processes, it is shown that the efficiency of the classification process increases with increasing particle concentration in the feed, as measured by an increasing fraction of smaller or slower-settling particles partitioning to the fine fraction rather than contaminating the coarse fraction. This is a direct result of hindered settling, which reduces the settling rate and increases the relative concentration of slower-settling particles in the upper portion of the vessel. Experimental data are presented for bidisperse suspensions of glass and acrylic beads and of coal particles and yeast cells, and for polydisperse suspensions of polystyrene latex beads. The results are in good agreement with the model predictions. Copyright © 1996 Elsevier Science Ltd.

Key Words: sedimentation, inclined settlers, hindered settling, particle classification

1. INTRODUCTION

In a variety of applications involving suspensions of small particles in fluids, it is desirable to classify or separate the particles based on differences in size or density. An attractive possibility for accomplishing the desired separation is the use of sedimentation vessels with inclined walls (Hill *et al.* 1977; Acrivos & Herbolzheimer 1979; Leung & Probstein 1983; Davis *et al.* 1989). Such vessels allow for large separation rates because of the short settling distances and the large surface areas available for sedimentation. Particles settle onto the upward-facing surface of each plate and slide down to the bottom of the settler where they are collected. The basic operation of inclined settlers, along with mathematical models and experimental verification, is described in the review by Davis & Acrivos (1985).

A continuous inclined settler for classifying particles according to size and/or density due to their different settling velocities is shown in figure 1. A feed suspension containing a mixture of particles is introduced near the bottom of the vessel. The underflow contains the coarse fraction enriched in faster-settling particles, whereas the overflow contains the fine fraction of slower-settling particles.

The basic theory describing the use of an inclined settler for classifying a dilute suspension of particles into fine and coarse fractions is presented by Davis *et al.* (1989). In their analysis, it was assumed that each particle sedimented with its isolated settling velocity. Good agreement between theory and experiment was obtained for feed concentrations of less than 1% particles by volume. In concentrated suspensions, however, we expect that particle–particle interactions affect the settling velocities of individual particles and, hence, the separation process. The present analysis and corresponding experiments focus on the effects of increasing particle concentration.

The sedimentation of concentrated bidisperse suspensions in inclined settlers has been studied previously by MacTaggart *et al.* (1988) and Nasr-El-Din *et al.* (1990) for the special case of one particle species being lighter than the fluid and the other species being heavier than the fluid. At the highest concentrations studied, fingering or lateral segregation of the two species was observed.

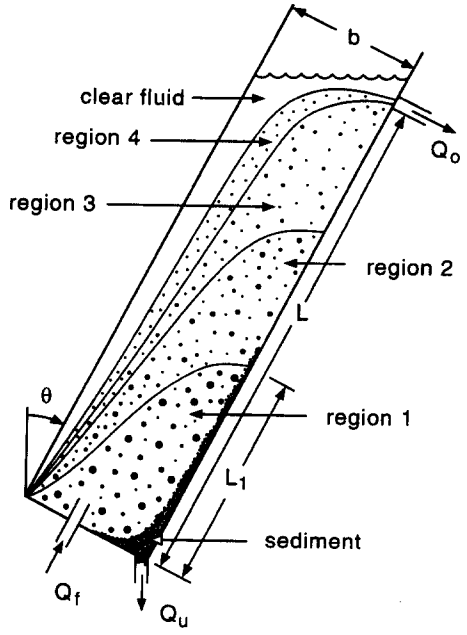

Figure 1. Schematic of an inclined settler containing four particle species, with an overflow rate such that only the two slowest-settling species reach the overflow.

This instability phenomenon for vertical settlers was first reported by Whitmore (1955) and has more recently been analyzed by Batchelor & Janse van Rensburg (1986). The key findings are that instabilities first occur when the combined particle concentration exceeds about 18% by volume and when the light and heavy particles are equal in size and have densities which are an equal amount below and above the fluid density, respectively. When the particles are of different sizes or are both heavier or both lighter than the fluid, then much higher concentrations are required for the instability to be observed, if at all. For two particle species with the same density, the analysis of Batchelor & Janse van Renburg (1986) predicts that the bidisperse suspension will be stable for all particle concentrations and size ratios. The present analysis is restricted to stable systems, and no fingering was observed in the experiments described.

2. THEORETICAL DEVELOPMENT

A continuous distribution of particles may be discretized into N species, with each species i characterized by its radius a_i and density ρ_i. This discretization has been shown to resolve typical distributions using $N = 10$ or greater (Smith 1966; Davis & Hassen 1988). A feed suspension containing N particle species will distribute into N suspensions regions, plus a sediment region below and a clarified fluid region above, when introduced in an inclined settler (Davis *et al.* 1982). This is illustrated in figure 1 for $N = 4$. Region 1 contains all particles, whereas the region immediately above is devoid of the fastest-settling species. Since each region is devoid of the fastest-settling species from the region below, region N contains only the slowest-settling particle species.

Continuity requires that the particle volume fractions in region 1 are the same as those in the feed stream (Davis *et al.* 1982):

$$\phi_{i,1} = \phi_{i,f}, \quad i = 1, 2, \ldots, N, \qquad [1]$$

where $\phi_{i,1}$ and $\phi_{i,f}$ are the volume fraction of species i in region 1 and in the feed suspension, respectively. The particle species are numbered such that species k is the fastest settling species in region k. The particle volume fraction in each region can be calculated by using the particle-flux continuity equation (Smith 1966):

$$\phi_{i,k+1}(v_{k,k} - v_{i,k+1}) = \phi_{i,k}(v_{k,k} - v_{i,k}), \quad i = k+1, \ldots, N; k = 1, \ldots, N-1, \qquad [2]$$

where $\phi_{i,k}$ and $v_{i,k}$ are the volume fraction and vertical settling velocity of species i in region k, respectively. Note that region $k+1$ is devoid of particles which settle faster than species $k+1$, and so

$$\phi_{i,k+1} = 0, \quad i = 1, 2, \ldots, k. \tag{3}$$

The vertical settling velocity of each particle species is given by its isolated settling velocity multiplied by a hindered settling function which depends on the local concentrations of the various particle species:

$$v_{i,k} = u_i^\circ f_{i,k}, \tag{4}$$

where $f_{i,k}$ is the hindered settling function for species i in region k. The settling velocity of an isolated spherical particle is given by Stokes law:

$$u_i^\circ = 2(\rho_i - \rho)a_i^2 \boldsymbol{g}/9\mu, \tag{5}$$

where a_i and ρ_i are the radius and density of particles of species i, respectively, ρ and μ are the fluid density and viscosity, respectively, and $\boldsymbol{g}$ is the gravitational acceleration. Equation [5] applies for small Reynolds number: $\mathrm{Re} = \rho u_i^\circ a_i/\mu \ll 1$. It is also assumed that the particles are larger than a few microns in diameter, so that the Péclet number is large and Brownian diffusion is negligible.

A simple hindered settling function with no empirical parameters, and which shows good agreement with a variety of experiments, is used (Davis & Gecol 1994):

$$f_{i,k} = (1 - \phi_k)^{C_{ii}}\left(1 + \sum_{j \neq 1} (C_{ij} - C_{ii})\phi_{j,k}\right), \tag{6}$$

where $\phi_k = \Sigma_i \phi_{i,k}$ is the total particle volume fraction in region k, and values for the sedimentation coefficients C_{ij} are given by the theory of Batchelor & Wen (1982). This function agrees with the theory of Batchelor (1982) for semidilute suspensions:

$$f_{i,k} = 1 - \sum_j C_{ij}\phi_{j,k} + O(\phi_k^2), \tag{7}$$

where the sedimentation coefficients C_{ij} depend on the size ratio $\lambda = a_j/a_i$ and the buoyant density ratio $\gamma = (\rho_j - \rho)/(\rho_i - \rho)$. The numerical values presented by Batchelor & Wen (1982) for equidensity non-colloidal particles ($\gamma = 1$) were fit to a polynomial over the range $0 \leqslant \lambda \leqslant 8$ (Davis & Gecol 1994):

$$C_{ij} = 3.50 + 1.10\lambda + 1.02\lambda^2 + 0.002\lambda^3. \tag{8}$$

Equation [6] reduces to the oft-used correlation of Richardson & Zaki (1954) for monodispersed suspensions:

$$f_{i,k} = (1 - \phi_k)^n, \tag{9}$$

provided that $n = C_{ii}$ is chosen. Note that $C_{ii} = 5.6$ for non-Brownian particles of equal densities and nearly equal size (Batchelor & Wen 1982), which is close to the value of $n = 5.1$ found from fitting [9] to experiments for monodisperse suspensions (Davis & Birdsell 1988). Equation [6] is expected to apply only to stable suspensions in the absence of lateral segregation or fingering.

The volume fraction and settling velocity of each particle species in each region is calculated by starting with $k = 1$, since the particle volume fractions in region 1 are known from [1], and then solving [2] for the particle volume fractions in region 2. This is repeated for each region and requires the simultaneous solution of $N - k$ coupled, non-linear algebraic equation sets.

According to the inclined settling theory for polydisperse suspensions (Davis *et al.* 1982), the clarification rate for region k, which is defined as the rate at which suspension crosses the interface separating region k and the region above it, is equal to the vertical settling velocity of the fastest-settling species in region k multiplied by the horizontal projection of the interface area. For the rectangular geometry of figure 1, this is given by

$$S_k = v_{k,k} w(L_k \sin\theta + b\cos\theta), \tag{10}$$

where w is the width of the channel, b is the spacing between the inclined walls, θ is the angle of inclination from the vertical and L_k is the length from the bottom of the channel up to the top of region k (see figure 1). The value of L_k increases with increasing overflow rate, Q_o. The maximum

value, $L_k = L$, occurs when $Q_o \geqslant S_{k,\max}$, where $S_{k,\max}$ is given by [10] with $L_k = L$. When this condition is met, region k spans the channel from top to bottom and partially enters the overflow.

Once the particle volume fractions and settling velocities are known for each region, they may be used together with macroscopic mass balances to predict the performance of the inclined settler/classifier. Mass balances on total suspension, total particles, and particles of species i about the entire settler at steady state are, respectively,

$$Q_f = Q_o + Q_u, \quad [11]$$

$$Q_f \phi_f = Q_o \phi_o + Q_u \phi_u, \quad [12]$$

$$Q_f \phi_{i,f} = Q_o \phi_{i,o} + Q_u \phi_{i,u}, \quad i = 1, 2, \ldots, N, \quad [13]$$

where Q refers to a volumetric flow rate, and the subscripts f, o and u refer to the feed, overflow and underflow streams, respectively.

In addition, a mixing-point mass balance is needed for each particle species entering the overflow. Consider the general case where the overflow rate is chosen such that $S_{m,\max} \leqslant Q_o < S_{m-1,\max}$, so that a portion of region m and all of regions $m + 1$ to N enter the overflow (this is shown schematically in figure 1 for $m = 3$, $N = 4$). Then, the mixing-point mass balance for each particle species entering the overflow stream is

$$Q_o \phi_{i,o} = (Q_o - S_{m,\max})\phi_{i,m} + \sum_{k=m+1}^{N} (S_{k-1,\max} - S_{k,\max})\phi_{i,k}, \quad i = m, \ldots, N, \quad [14]$$

where $Q_o - S_{m,\max}$ is the rate at which region m enters the overflow and $S_{k-1,\max} - S_{k,\max}$ is the rate at which region k enters the overflow. Since the regions below region m do not reach the overflow, particles which settle faster than species m are not present in the overflow:

$$\phi_{i,o} = 0 \quad i = 1, 2, \ldots, m - 1. \quad [15]$$

Once $\phi_{i,o}$ is found for all species, $\phi_{i,u}$ is determined from [13], and the total particle volume fractions in the overflow (ϕ_o) and underflow (ϕ_u) are determined by summing over the individual species.

3. MATERIALS AND METHODS

3.1. Bidisperse suspensions

Two bidisperse systems were used. The first contained a mixture of spherical glass particles (Ferro Corporation) of density $\rho_1 = 2.49\ \text{g/cm}^3$ and median diameter (volume basis) of $2a_1 = 267\ \mu\text{m}$ and spherical acrylic particles (Imperial Chemistry Industries) of density $\rho_2 = 1.183\ \text{g/cm}^3$ and median diameter $2a_2 = 83\ \mu\text{m}$. These particles were suspended in a Newtonian hydrocarbon fluid UCON 50 HB-280X (Union Carbide) of density $\rho = 1.034\ \text{g/cm}^3$ and viscosity $\mu = 1.13$ g/cm-s at 25°C. The particle sizes were measured with a Coulter Multisizer, and their densities were measured by blending fluids to find the neutral density. The fluid viscosity was measured with a capillary-tube viscometer (Cannon) and the fluid density was measured with a hydrometer. Although the particles were sieved prior to use, they each exhibited a distribution of sizes; figure 2 shows the cumulative distribution functions for these particles, defined such that $F(D)$ is the fraction of particles by volume with diameters less than D.

The second suspension consisted of a mixture of yeast cells (a sulfur-utilizing strain of unknown genus provided by Dr J. R. Mattoon of the University of Colorado, Colorado Springs, CO 80933-7150, U.S.A.) and pulverized coal (Illinois No. 6 bituminous coal) in deionized water at pH 7 and 30°C ($\rho = 0.996\ \text{g/cm}^3$, $\mu = 0.00827$ g/cm-s). This suspension was chosen because of its potential application in microbial disulfurization of coal. The cumulative size distributions of the cells and particles are shown in figure 3. The median diameters of these particles are $2a_1 = 62.4\ \mu\text{m}$ and $2a_2 = 4.73\ \mu\text{m}$ for coal and yeast, respectively, with the respective densities being $\rho_1 = 1.31\ \text{g/cm}^3$ and $\rho_2 = 1.05\ \text{g/cm}^3$.

The inclined settler employed for the glass/acrylic particles was fabricated from Plexiglas and has dimensions $L = 60$ cm, $b = 2.5$ cm and $w = 3.5$ cm. The angle of inclination from the vertical was set at $\theta = 45°$, which provided a large sedimentation rate and yet allowed for the sediment to

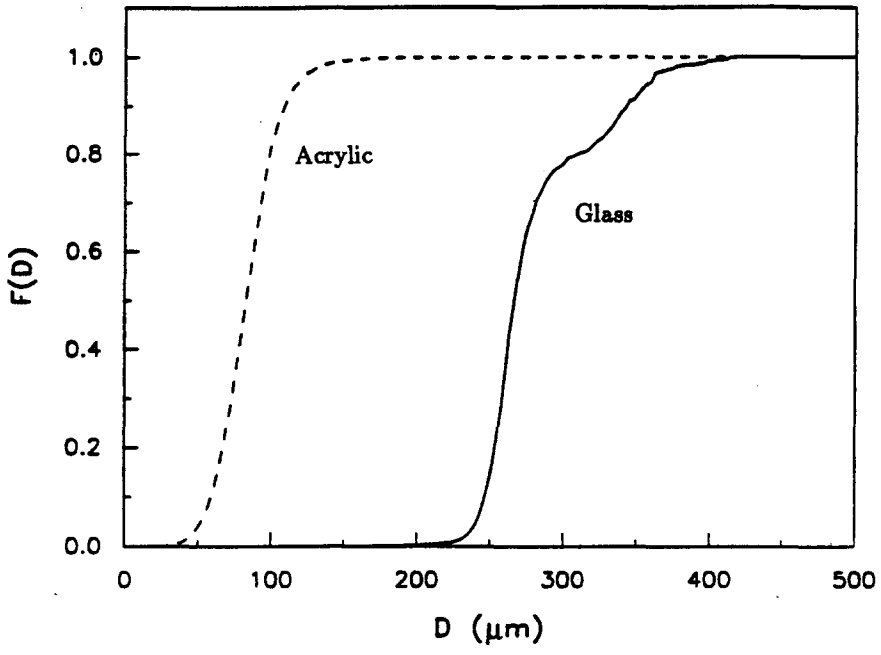

Figure 2. Cumulative size distribution functions for acrylic (dashed curve) and glass (solid curve) particles.

easily slide down the upward-facing wall to the bottom of the settler. An open-bottom design was used (Davis *et al.* 1989), so that the sediment layer slid down the lower wall of the channel directly into the 4-l feed reservoir controlled at 25°C. A peristaltic pump was used to draw suspension up through the settler at a controlled overflow rate. The overflow was recycled (except for occasional small samples) to the feed reservoir in order to maintain steady concentrations.

The glass particle volume fraction in the feed reservoir was held fixed at $\phi_{1,f} = 0.05$. The acrylic particle volume fraction was varied: $\phi_{2,f} = 0.05$, 0.15 and 0.25. For each concentration, seven

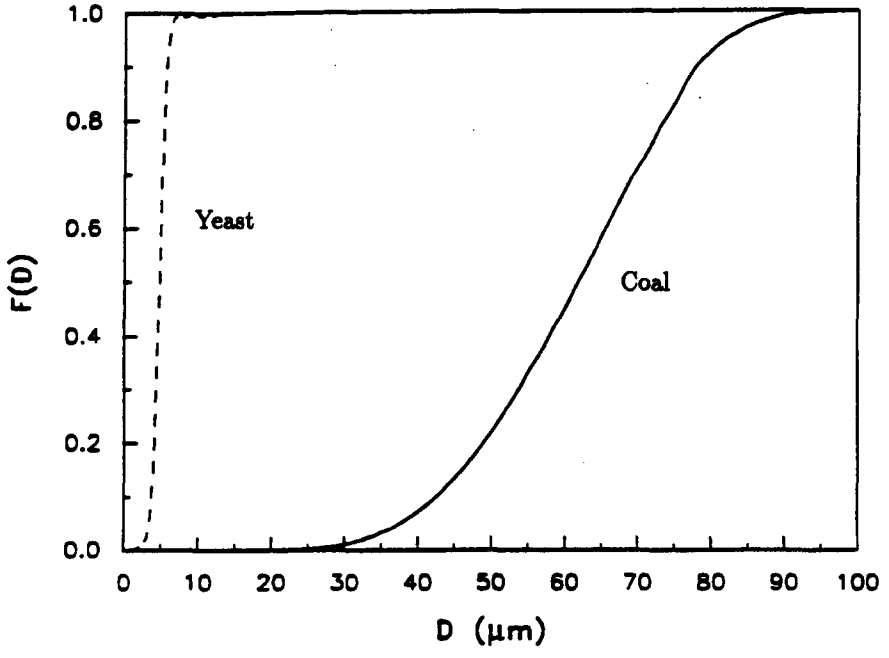

Figure 3. Cumulative size distribution functions for yeast (dashed curve) and coal (solid curve) particles.

Table 1. Settling properties of the different particle types

Particles	$u_{i,o}$ (cm/min)	Re	$S_{i,o}$ (cm^3/min)
Glass	0.3	1.2×10^{-3}	464
Acrylic	0.0030	3.8×10^{-6}	4.64
Coal	4.9	6.1×10^{-2}	228
Yeast	0.0048	4.6×10^{-6}	0.224
Latex	0.67	7.3×10^{-3}	103

overflow rates within the range 1 cm^3/min $< Q_o <$ 90 cm^3/min were used, and each experiment was repeated three times. After steady state was reached (1–2 h), several samples from the overflow line and the feed reservoir were taken and analyzed by using density-separation of the two particle species and then drying and weighing the fractions. Further details of the experimental procedures are given by Gecol (1992).

The inclined settler employed for the coal/yeast experiment was fabricated from rectangular glass tubing and has dimensions $L = 16$ cm, $b = 0.5$ cm and $w = 4$ cm, and its angle of inclination was chosen to be $\theta = 45°$. Unlike for the glass/acrylic particles, a peristaltic pump was used to control the underflow rate, with the value fixed at $Q_u = 4.95$ cm^3/min. Another peristaltic pump controlled the overflow rate, with values of $Q_o = 0.34$, 0.64 and 2.26 cm^3/min employed. Both the underflow and overflow were recycled (except for sampling) to the 1.5-l feed reservoir, which was temperature controlled at 30°C. The settler also was controlled at 30°C, using a glass water jacket.

The volume fractions of coal and yeast particles in the feed were fixed at $\phi_{1,f} = \phi_{2,f} = 0.05$. The yeast cells were prepared by growing them in a rich medium and then harvesting them from the fermentor by centrifugation and storing them in a glycerin solution at 4°C until ready for use. The cells remained viable during the sedimentation experiments, and their concentrations in the feed, underflow and overflow were determined by plating diluted samples on Petri dishes containing agar and growth medium. The volume fraction of coal particles was determined by weighing dried samples and subtracting the dry cell weight. Further details are given by Gecol (1992).

Table 1 lists the Stokes velocity, the corresponding Reynolds number, and the characteristic clarification rate (where $S_{i,o}$ is given by [10] with $L_k = L$ and $v_{k,k} = u_{i,o}$) for the median-sized particle of each type in its respective suspending fluid and settler. Note that, in all cases, the Reynolds number is small compared to unity.

3.2. Polydisperse suspensions

Experiments were also performed with a monomodal suspension of polystyrene latex beads (Dow Chemical) of density $\rho_i = 1.049$ g/cm^3 in water at 25°C ($\rho = 0.987$ g/cm^3 and $\mu = 0.0089$ g/cm-s), with 10 drops of Triton X-100 per liter to help disperse the particles and five drops of bleach per liter to prevent microbial growth. The normalized probability density function of particle diameters, $P(D) = dF/dD$, is shown in figure 4 (volume basis). The median diameter is $D_m = 59$ μm, with a standard deviation of 12 μm. The size distribution was measured with an Elzone 180 XY (Particle Data Systems). Also shown in figure 4 is the "theoretical" feed distribution, which is simply the normal probability distribution having the same mean and standard deviation as the measured distribution.

The inclined settler and feed reservoir employed are the same as those used for the bidisperse suspensions of glass and acrylic particles. The angle of inclination was again kept at $\theta = 45°$. The settling parameters for the median particle size are given in table 1. Experiments were performed with total feed particle volume fractions of $\phi_f = 0.01$, 0.10, 0.20 and 0.40. Six overflow rates were used for each feed suspension, and each experiment was repeated twice. Samples were taken from the overflow line and feed reservoir after steady state was reached, and analyzed by the Elzone 180 XY for the particle size distributions. A drying and weighing procedure was used to determine particle concentrations.

4. RESULTS AND DISCUSSION

4.1. Bidisperse suspensions

Figure 5 shows the results for the dimensionless concentration of the acrylic particles in the overflow versus the dimensionless overflow rate for the three feed concentrations. In all exper-

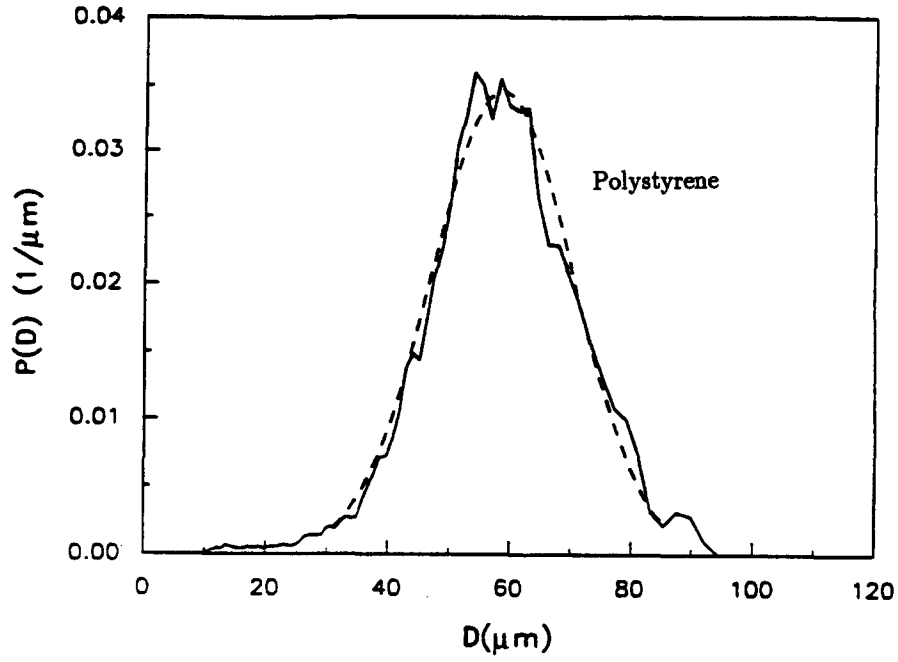

Figure 4. Normalized probability density function for polystyrene latex beads; the solid curve is from the measurements, and the dashed curve is a fitted normal probability function.

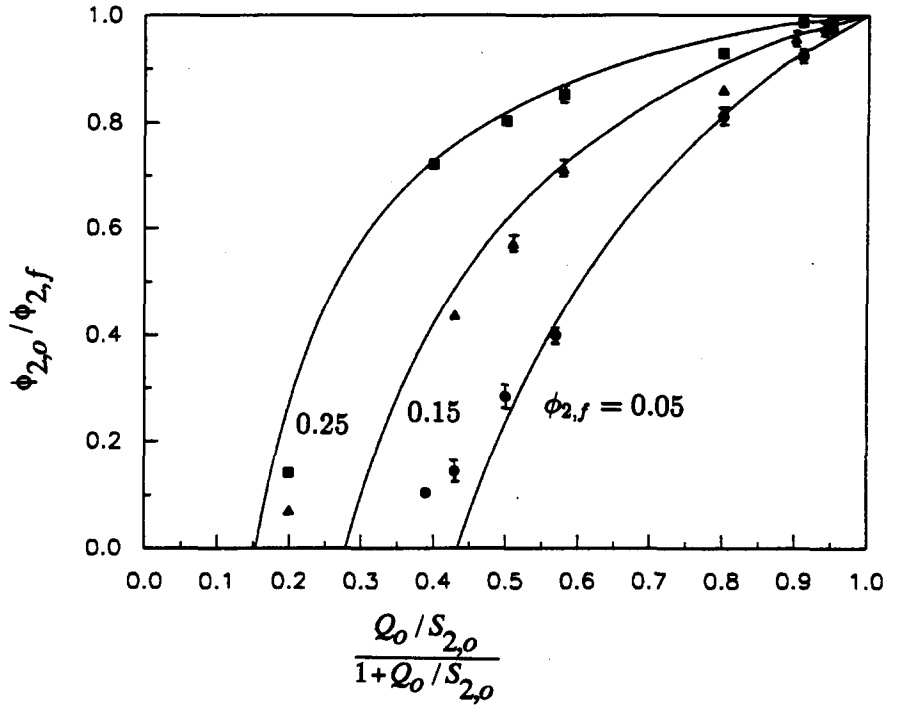

Figure 5. The relative concentration of acrylic beads in the overflow as a function of the dimensionless overflow rate for $\phi_{1,f} = 0.05$ and $\phi_{2,f} = 0.05$, 0.15 and 0.25 (right to left). The solid lines are theoretical predictions and the symbols are experimental data. The error bars are 90% confidence limits about the mean.

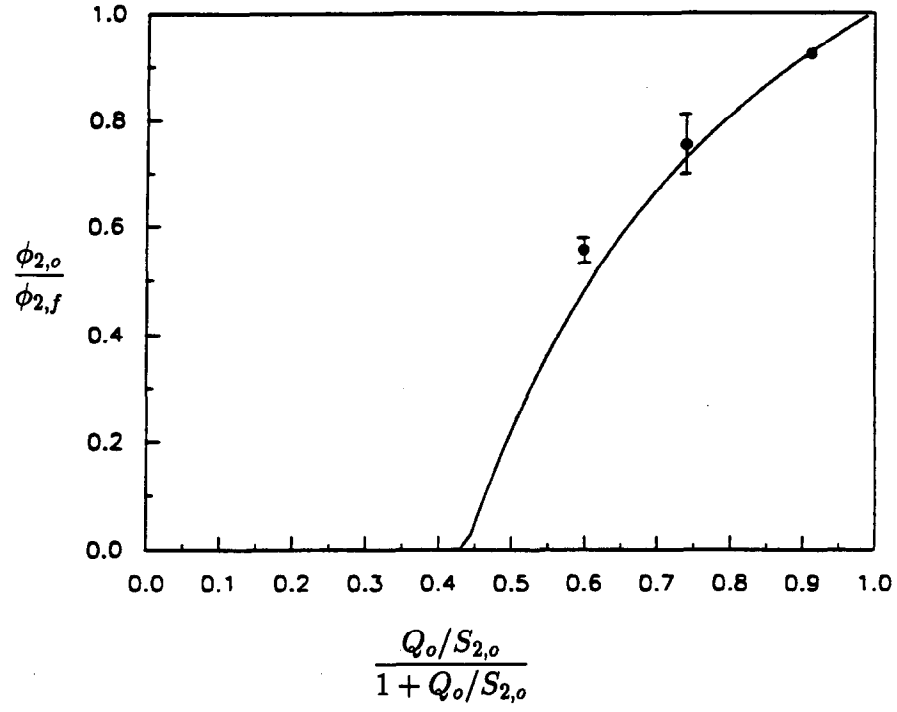

Figure 6. The relative concentration of yeast cells in the overflow for $\phi_{1,f} = \phi_{2,f} = 0.05$; the symbols are the measured means with the 90% confidence limits shown, and the solid curve is theory.

iments, no glass particles were observed to reach the overflow. Both the experimental data and the theory show that the concentration of the slower-settling particles in the overflow stream increases as the volumetric overflow rate is increased. This is due to there being less holdup time for settling at higher overflow rates. At sufficiently low overflow rates, all particles are predicted to settle before reaching the overflow ($L_2 < L$) and so $\phi_{2,o} = 0$. In general, there is very good agreement between theory and experiment. An exception is at very low feed concentrations and overflow rates, for which more of the slower-settling particles reach the overflow than predicted. This is due to the polydispersity of the acrylic particles, with particles smaller than the median size reaching the overflow at low overflow rates. This has been verified using a Coulter Multisizer to measure the particle size distributions in the samples (Gecol 1992). The theory curves in figure 5 were generated using the following values for the sedimentation coefficients: $C_{11} = C_{22} = 5.6$, $C_{12} = 2.6$, and $C_{21} = 205$ (Batchelor & Wen 1982). Note that theoretical calculations treated the glass and acrylic particles as single species, each characterized by its density and median particle diameter, despite the measured distribution of sizes within each particle type (figure 2).

A particularly relevant result from the data and theory shown in figure 5 is that the fractional recovery of the acrylic beads in the overflow product line increases with increasing volume fraction of acrylic beads in the feed stream. This is because the particles settle more slowly at higher concentrations and so a greater fraction of them reach the overflow without settling out of suspension. Moreover, the ratio of the concentration of the acrylic particles in region 2 to that in region 1 increases with increasing concentration due to hindered settling, as required by the particle flux continuity equation [1]. Thus, classification by inclined settling is one of the few processes which becomes more efficient with increasing concentration.

Figure 6 shows the relative concentration of yeast cells in the overflow stream as a function of the overflow rate. As expected, the recovery increases with increasing overflow rate, with less than 10% of the yeast cells sedimenting out of suspension for the highest rate. In contrast, no coal particles were observed in the overflow for the two lowest overflow rates, and a relative concentration of only $\phi_{1,o}/\phi_{1,f} = 0.03$ was measured for the highest overflow rate. The few coal

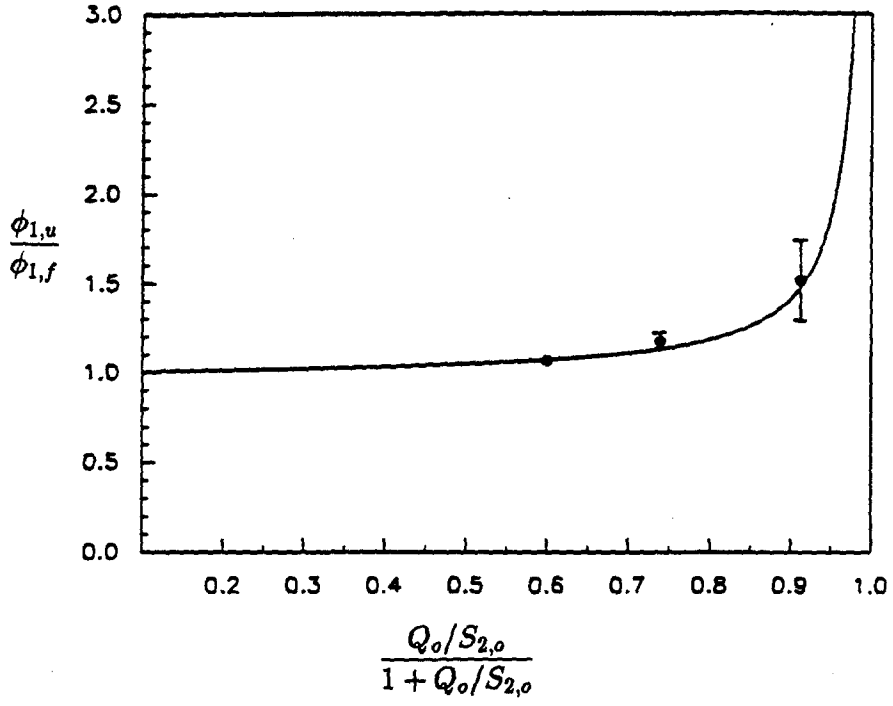

Figure 7. The relative concentration of coal particles in the underflow for $\phi_{1,f} = \phi_{2,f} = 0.05$; the symbols are the measured means with the 90% confidence limits shown, and the solid curve is theory.

particles that did reach the overflow were observed to be much smaller than the median size. Thus, a very good separation of coal from yeast in the fine fraction was achieved.

Figure 7 shows the relative coal concentration in the underflow (coarse fraction) stream. This concentration increased with increasing overflow rate, since the underflow rate was held fixed and

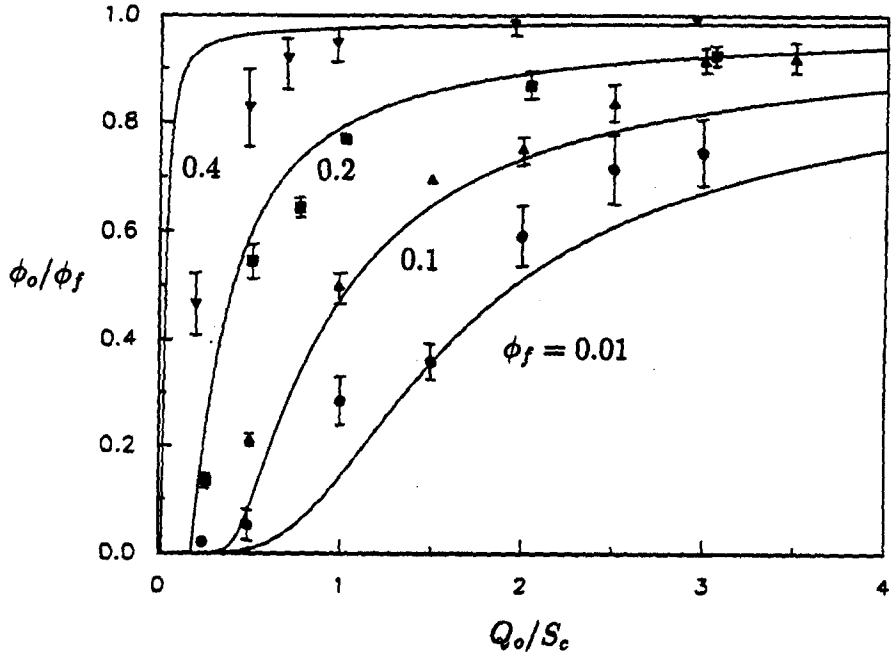

Figure 8. The total relative concentration of polystyrene latex particles in the overflow for total feed volume fractions of $\phi_f = 0.01$, 0.10, 0.20 and 0.40 (bottom to top); the symbols are experimental data with the 90% confidence limits shown, and the solid curves are theory.

the feed rate increased with increasing overflow rate. Again, the data are in good agreement with theory. The yeast concentration in the underflow was only slightly (<5%) higher than that in the feed, since the settler was designed for relatively little sedimentation of the yeast cells.

4.2. Polydisperse suspensions

Figure 8 is a plot of the total volume fraction of particles in the overflow, relative to that in the feed, versus the dimensionless overflow rate, Q_o/S_c, for total feed volume fractions of $\phi_f = 0.01$, 0.10, 0.20 and 0.40. The characteristic rate S_c is given by [10] with $L_k = L$ and $v_{k,k}$ replaced by the Stokes velocity of a particle with the median diameter D_m. As with the bidisperse experiments, the fractional recovery of particles in the fine fraction (overflow) increased with increased overflow rate, due to the decreased holdup time in the settler. For a given overflow rate, the particle recovery in the overflow increased with increased feed volume fraction, due to hindered settling reducing the sedimentation rate. The experiments are generally in good agreement with the theory, except that more particles than predicted reached the overflow at low volume fractions, and fewer particles than predicted reached the overflow at high volume fractions. For low volume fractions, instabilities were observed along the interface separating the thin layer of clarified fluid beneath the downward-facing inclined surface and the suspension (see figure 1), and along the interface separating the thin sediment layer above the upward-facing inclined surface and the suspension (see figure 1). These instabilities caused remixing of clarified fluid and settled particles, respectively, which reduced the efficiency of the inclined settling process and led to more particles reaching the overflow. Such instabilities have been studied previously by Herbolzheimer (1983), Davis *et al.* (1983) and Borhan (1989), among others, who showed that increasing the particle volume fraction (above some small value) stabilizes the flow. Consistent with theoretical predictions, the instabilities were not observed at the two highest particle volume fractions. The poor agreement between theory and experiment for the most concentrated suspension at low overflow rates may be a result of the loss of accuracy of the proposed hindered settling law at very high concentrations; in particular, the particles may lock together and not be able to settle differentially, at particle volume fractions greater than about 0.3.

The measured particle size distributions in the overflow stream provide further support of the mechanisms discussed above. As shown in figure 9, the mean particle diameter in the overflow

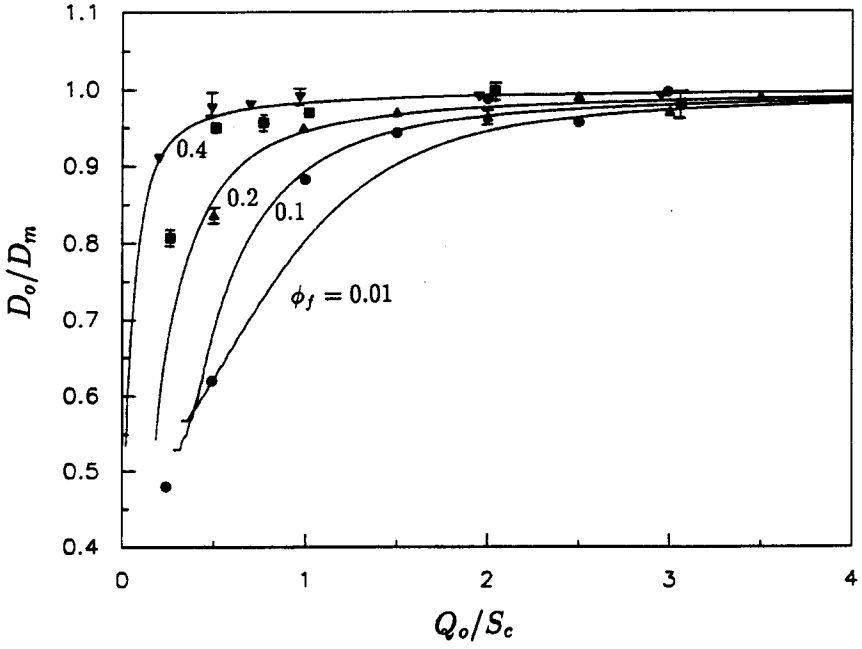

Figure 9. The relative mean particle diameter of polystyrene latex particles in the overflow for total feed volume fractions of $\phi_f = 0.01$, 0.10, 0.20 and 0.40 (bottom to top); the symbols are experimental data with the 90% confidence limits shown, and the solid curves are theory.

increased with increasing overflow rate; this again is a result of decreased holdup time which allowed larger particles to reach the overflow before settling out of suspension. The data at low overflow rates are slightly higher than the theoretical predictions. This is likely a result of dispersion, neglected in the analysis, which might arise from the instabilities discussed above or from hydrodynamnic diffusion due to particle–particle interactions (Davis & Hassen 1988).

The theoretical results shown in figures 8 and 9 were made by assuming a normal probability density function with the same mean diameter and standard deviation as those measured by the Elzone 180 XY (see figure 4). This size distribution was discretized over the range of plus and minus 2.5 standard deviations about the mean. A value of $N = 25$ was found to be sufficient to describe the continuous distribution and produce results which converged within 0.1% (Davis & Hassen 1988). Equation [8] was used for the sedimentation coefficients.

5. CONCLUDING REMARKS

An inclined settler is capable of classifying (separating) particles on the basis of differential settling due to differences in particle sizes and/or densities. When a feed suspension is fed into an inclined settler at an appropriately chosen rate, the faster-settling particles will sediment onto the upward-facing surfaces and partition primarily to the coarse-fraction underflow, whereas the overflow contains primarily particles which sediment slower than the overflow rate divided by the horizontal projection of the area available for settling. As the particle volume fraction in the feed is increased, hindered settling becomes important. A direct effect of the hindered setting is that the particles sediment more slowly and so a greater fraction of particles reach the overflow stream. Another effect of inclined settling is that the concentrations of the slower-settling particles are higher in the upper regions of the settler than in the feed or lower regions, which also causes a greater fraction of the slower-settling particles to reach the overflow. Thus, if the goal is to separate slower-settling (e.g. smaller) particles from the others, then the efficiency of the process is improved by increasing the feed concentration—provided that the overflow rate is chosen so that the undesired faster-settling particles do not reach the overflow stream to an appreciable extent.

Acknowledgement—This work was supported by NSF Grant BCS-8912259. The assistance of Dawn Downey and the University of Colorado's Undergraduate Research Opportunities Program is gratefully acknowledged.

REFERENCES

Acrivos, A. & Herbolzheimer, E. 1979 Enhanced sedimentation of settling tanks with inclined walls. *J. Fluid Mech.* **90,** 435–457.

Batchelor, G. K. 1982 Sedimentation in a dilute polydisperse system of interacting spheres: 1. General theory. *J. Fluid Mech.* **119,** 379–408.

Batchelor, G. K. & Janse van Rensburg, R. W. 1986 Structure formation in bidisperse sedimentation. *J. Fluid Mech.* **166,** 379–407.

Batchelor, G. K. & Wen, C. S. 1982 Sedimentation in a dilute polydisperse system of interacting spheres: 2. Numerical results. *J. Fluid Mech.* **124,** 495–528.

Borhan, A. 1989 An experimental study of the effect of suspension concentration on the stability and efficiency of inclined settlers. *Phys. Fluids A* **1,** 108–123.

Davis, R. H. & Acrivos, A. 1985 Sedimentation of noncolloidal particles at low Reynolds numbers. *Ann. Rev. Fluid Mech.* **17,** 91–118.

Davis, R. H. & Birdsell, K. H. 1988 Hindered settling of semidilute monodisperse and polydisperse suspensions. *AIChE J.* **34,** 123.

Davis, R. H. & Gecol, H. 1994 Hindered settling of function with no empirical parameters for polydisperse suspensions. *AIChE J.* **40,** 570–575.

Davis, R. H. & Hassen, M. A. 1988 Spreading of the interface at the top of a slightly polydisperse sedimenting suspension. *J. Fluid Mech.* **196,** 107–134.

Davis, R. H., Herbolzheimer, E. & Acrivos, A. 1982 Sedimentation of polydisperse suspensions in vessels having inclined walls. *Int. J. Multiphase Flow* **8,** 571–585.

Davis, R. H., Herbolzheimer, E. & Acrivos, A. 1983 Wave formation and growth during sedimentation in narrow tilted channels. *Phys. Fluids* **26,** 2055–2064.

Davis, R. H., Zhang, X. & Agarwala, J. P. 1989 Particle classification for dilute suspensions using an inclined settler. *Ind. Engng Chem. Res.* **28,** 785–793.

Gecol, H. 1992 A novel bioreactor/separator for microbial desulfurization of coal. M.Sc. thesis, University of Colorado, Boulder, CO, U.S.A.

Herbolzheimer, E. 1983 The stability of the flow during sedimentation beneath inclined surfaces. *Phys. Fluids* **26,** 2043–2054.

Hill, W. D., Rothfus, R. R. & Li, K. 1977 Boundary-enhanced sedimentation due to settling convection. *Int. J. Multiphase Flow* **3,** 561–583.

Leung, W. F. & Probstein, R. F. 1983 Lamella and tube settlers. I. Model and operation. *Ind. Engng Chem. Proc. Des. Dev.* **22,** 58–67.

MacTaggart, R. S., Hin-Sum Law, D., Masliyah, J. H. & Nandakumar, K. 1988 Gravity separation of concentrated bidisperse suspensions in inclined plate settlers. *Int. J. Multiphase Flow* **14,** 519–532.

Nasr-El-Din, H. A., Masliyah, J. H. & Nandakumar, K. 1990 Continuous gravity separation of concentrated bidisperse suspensions in an inclined plate settler. *Int. J. Multiphase Flow* **16,** 909–919.

Richardson, J. F. & Zaki, W. N. 1954 Sedimentation and fluidization: I. *Trans. Inst. Chem. Engng* **32,** 35.

Smith, T. N. 1966 The sedimentation of particles having a dispersion of sizes. *Trans. Inst. Chem. Engng* **44,** T153–T157.

Whitmore, R. L. 1995 The sedimentation of suspensions of spheres. *Br. J. Appl. Phys.* **6,** 239–245.